Neural Networks provide a good alternative to classical FD method. They are able to rapidly and accurately solve the task.

Waveform and interferences are well reproduced and the net manages to predict multiple reflections, which are not directly linked to the interface position.

We propose also a method based on retraining to reduce this problem. This method gives good results and it is able to make adjustments of the net parameters in a short time (less than one hour on ENI's HPC4) and with a small dataset.

This technique may open new perspectives of development: future research could test the net in the elastic 1-D approximation prediction and in the solution of 2-D direct and inverse problems.

Acknowledgements. The first author wishes to acknowledge ENI SpA for their assistance and for allowing him the use of their computer cluster (HPC4). The Devito project [2] is also acknowledged for the highly optimized finite difference kernels used in this work.

References

[1] Hochreiter S. and Schmidhuber J.; 1997: *Long Short-term Memory*. Neural computation 9, pp. 1735–80.

[2] Louboutin M., Lange M., Luporini F., Kukreja N., Witte P. A., Herrmann F. J., Velesko P. and Gorman G. J.; 2019: *Devito (v3.1.0) an embedded domain-specific language for finite differences and geophysical exploration*. Geoscientific Model Development, Volume 12, p 1165-1187, 2019

[3] Murphy K. P.; 2012: *Machine learning : a probabilistic perspective* ISBN 978-0-262-01802-9, MIT Press.

[4] Sherstinsky A.; 2018: *Fundamentals of Recurrent Neural Network (RNN) and Long Short-Term Memory (LSTM) Network*. ArXiv abs/1808.03314.

A DATA-DRIVEN TRANSDIMENSIONAL INVERSION APPROACH TO INCLUDE LATERAL CONSTRAINTS INTO TARGET-ORIENTED AVA INVERSION

A. Salusti[1,2], M. Aleardi[2]

[1] University of Florence, Earth Sciences Department, Florence, Italy

[2] University of Pisa, Earth Sciences Department, Pisa, Italy

Introduction. The inclusion of lateral constraints into the inversion framework is the most popular strategy devoted at attenuating the ill-conditioning of the seismic inversion. The Tikhonov approach is by far the most popular regularization approach even if it has several disadvantages, for example this method often leads to unfocused layer transitions. Other more advanced regularization strategies exist, such as the inclusion of geostatistical constraints in the form of isotropic model correlation functions (Buland *et al*. 2003), or stratigraphic constraints (Tetyukhina *et al*. 2010). The main limit of all these approaches is that they rely on an a-priori structural knowledge of the investigated area and force the recovered model to honor such a-priori constraint. These are essentially model-driven regularization strategies that could provide biased model parameter estimations in case of erroneous a-priori assumptions. To overcome these issues more advanced, adaptive, regularization strategies have been proposed (e.g. Aleardi *et al*. 2018). The goal of these approaches is to locally adapt the structural constraint to the local structural characteristics of the subsurface model that can be iteratively inferred form the local characteristics (i.e. variability) of the observed data.

On the line of these data-driven approaches, we present a transdimensional reversible jump Markov Chain Monte Carlo (rjMCMC) algorithm for target-oriented amplitude versus angle

(AVA) inversion. In our case target-oriented means that only the AVA responses of the target layer are inverted, and these AVA responses are extracted for each considered CDP position. The results are 2D maps representing the lateral variability of the elastic contrasts along the considered reflecting interface. The AVA inversion is a severely ill-conditioned problem highly affected by noise contamination in which it is crucial adopting a reliable regularization strategy to retrieve reliable and stable results. In a transdimensional inversion the number of model parameters (that codes the optimal subsurface model parameterization) is considered unknown and is estimated using a probabilistic sampling. In our case the inverted 2D horizon is divided into Voronoi cells, whose number and shape are automatically determined by the rjMCMC sampling. The algorithm autonomously partitions the considered 2D horizon on the basis of the spatial variability of data, producing subsurface 2D models discretized in Voronoi polygons each one enclosing CDP positions with similar AVA responses. This also means that the CDPs falling within the same cell also share similar elastic properties and for this reason the same elastic property values are assigned to these CDPs. These values are computed by averaging the model properties pertaining to the CDPs falling within each cell. Similarly, the observed data for each polygon is computed by averaging the AVA responses of the CDPs falling within each Voronoi cell. From the one hand, this strategy constitutes a data-driven approach to include lateral constraints into the AVA inversion because these constraints are automatically inferred from the lateral variability of the data and not arbitrarily infused into the inversion framework. From the other hand, the averaging of the AVA responses pertaining to CDPs falling within the same cell inherently increases the signal-to-noise (S/N) ratio of the observed data. These two aspects revealed to be of crucial importance for stabilizing the inversion even in case of severely noise-contaminated data.

For the lack of field data, we test the implemented rjMCMC algorithm performing synthetic inversions with different S/N ratios. The proposed method is benchmarked against a more standard Bayesian AVA inversion without lateral constraints.

The method. In case of parameterizations with different number of unknowns n, the Bayes theorem can be written as (Bodin and Sambridge 2009):

$$p(\mathbf{m}, n \,|\, \mathbf{d}) = \frac{p(\mathbf{d} \,|\, \mathbf{m}, n) p(\mathbf{m} \,|\, n) p(n)}{p(\mathbf{d})} \tag{1}$$

where $\mathbf{d}$ is the observed data vector, and $\mathbf{m}$ is the model parameter vector. The left-hand side term of equation 1 is the target PPD that could be numerically estimated from the ensemble of models sampled by the MCMC algorithm. In a transdimensional rjMCMC, the Metropolis-Hasting rule that determines the acceptance probability α (that is the probability to move from a model $\mathbf{m}$ with dimension n to a model $\mathbf{m'}$ with dimension n' at a given step of the chain) becomes:

$$\alpha = p\left(\mathbf{m}', n' \,\middle|\, \mathbf{m}, n\right) = \min \left[1, \frac{p(\mathbf{m}', n')}{p(\mathbf{m}, n)} \times \frac{p(\mathbf{d} \,|\, \mathbf{m}', n')}{p(\mathbf{d} \,|\, \mathbf{m}, n)} \times \frac{q(\mathbf{m}, n \,|\, \mathbf{m}', n')}{q(\mathbf{m}', n' \,|\, \mathbf{m}, n)} \times \left|\mathbf{J}\right|\right], \tag{2}$$

where $\mathbf{J}$ is the Jacobian of the transformation from $\mathbf{m}$ to $\mathbf{m'}$ and is needed to account for the scale changes when the transformation involves a jump between models with different dimensions; $\boldsymbol{q}()$ is the proposal distribution that defines the new model $\mathbf{m'}$ as a random deviate from a probability distribution $q(\mathbf{m'}|\mathbf{m})$ conditioned only on the current model $\mathbf{m}$.

As the forward modelling we use the Ursenbach and Stewart equations (Ursenbach and Stewart, 2008) that constitutes an approximation of the exact Zoeppritz equations, parameterized in terms of relative contrasts in P-impedance and S-impedance (*RI* and *RJ*, respectively) at the reflecting interface. We discretize the investigated 2D horizon using the Voronoi polygons defined over equally spaced grid points representing the CDP positions. A discrete set of points, the center of the Voronoi cells, partitions the considered 2D horizon and each cell encloses the CDP gathers with the smallest distance from the center of the associated Voronoi polygons. The

inversion starts from a model drawn from the prior distribution; the model parameters include the number of Voronoi cells, the position of their nuclei, and the elastic properties associated to each polygon. All this a-priori information is uniformly distributed over a given parameter range, whereas the likelihood function is based on the L2 norm difference between observed and predicted AVA responses under the assumption of Gaussian distributed noise. To all the *N* CDP positions falling within the same cell are assigned the same elastic property values that are computed as the average of their *RI* and *RJ* values. Similarly, the average AVA response of the *N* CDPs constitute the observed data for the considered cell. Then the algorithm evolves by sampling the model space, that is by sampling the *RI* and *RJ* values, the number of cells, and the positions of their nuclei. The sampling is driven by the acceptance probability given in Eq. 2, in which models with better fit with the observed data and with a parsimonious parameterization (lower number of cells) are more likely to be accepted. During the iterations the algorithm tends to gather within the same Voronoi cell adjacent CDPs with similar AVA responses to which are assigned the elastic properties that produces a good fit with the observed data. At each iteration, the algorithm applies a perturbation to the current model chosen with equal probability from the following list:

1. *Birth move*: Create a new polygon within the Voronoi tessellation and assign the elastic properties to the newly created polygon by drawing a random realization from the prior *RI* and *RJ* distribution. Note that only the neighboring cells of the new-born cell have their geometry changed during this step.
2. *Death move*: Delete one polygon from the Voronoi tessellation and rearrange the shape of the remaining polygons based on the positions of their nuclei.
3. *Elastic move*: Randomly choose one Voronoi cell and perturb the *RI* and *RJ* values for all the CDP positions enclosed in the selected cell. This perturbation follows a Gaussian proposal centered on the current *RI* and *RJ* values.
4. *Cell move*: Randomly choose one Voronoi cell and change the position of the corresponding center without modifying the associated *RI* and *RJ* values. This perturbation will produce a slightly rearrangement of the Voronoi tessellation over the considered 2D horizon.

To increase the computational efficiency of the algorithm we employ a parallel tempering strategy in which multiple and interactive chains are simultaneously run at different temperature levels. High-temperature chains ensure a wide exploration of the model space, whereas low-

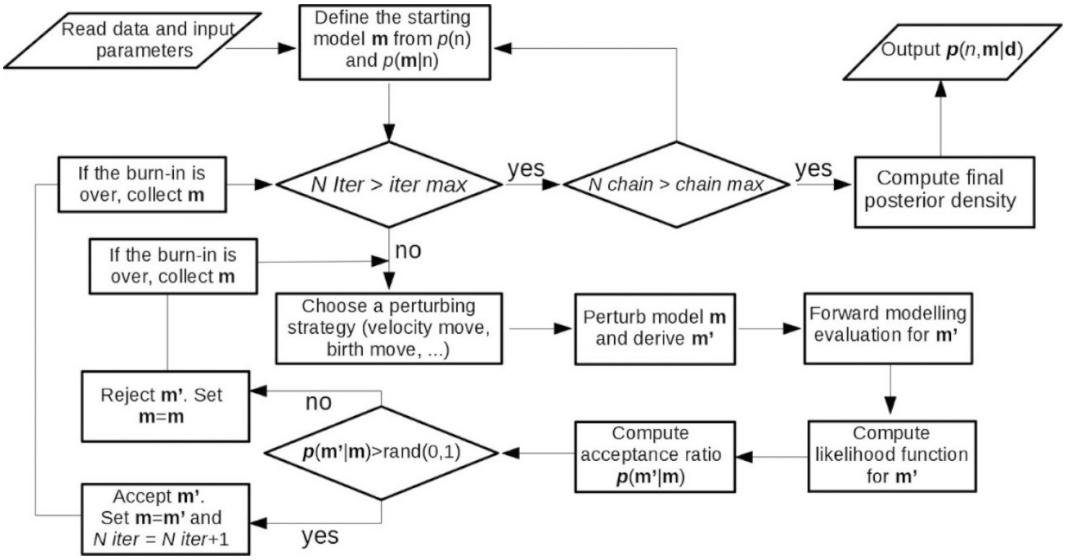

Fig. 1 - Schematic representation of the rjMCMC inversion.

temperature chains ensure exploitation of the high-probability regions. According to stochastic criteria, swaps of models are allowed between chains at different temperatures, and in this context the high temperature chains ensure that low-temperature chains access all the high probability regions while maintaining an efficient exploitation capability. Only the models collected at $T = 1$ are considered in the computation of the PPD because the models collected at $T > 1$ sample a biased posterior probability density function. Fig. 1 shows the flowchart of the implemented rjMCMC inversion, whereas Fig. 2 illustrates an example of evolution of the *RI* models sampled by the algorithm. These models represent the *RI* values estimated over a 2D stratigraphic horizon. We note that the algorithm starts from *RI* values very different from the reference model and from a Voronoi tessellation with a number of cells that is not enough to successfully predict the observed data. As the iterations proceed, the sampled *RI* values get closer to the reference model, whereas the Voronoi tessellation successfully partitions the considered 2D horizon by gathering within the same polygon CDPs with similar AVA response. In other terms, the algorithm successfully recognizes adjacent CDP positions with similar AVA responses and similar relative contrasts in the P- and S-impedance values.

Synthetic inversion tests. The synthetic observed AVA data are computed from a reference elastic model constituted by a regularly spaced grid of 160 x 240 CDPs. This reference model (leftmost part of Fig. 3) represents a stratigraphic section of a deltaic depositional area characterized by twisted river channel systems where yellow regions are representative of predominantly sandy channels, nested in blue-colored background shale portions with significant lateral contrasts in the *RI* and *RJ* values. The Ursenbach and Stewart equation is applied to the reference model to compute the AVA response for each CDP gather position

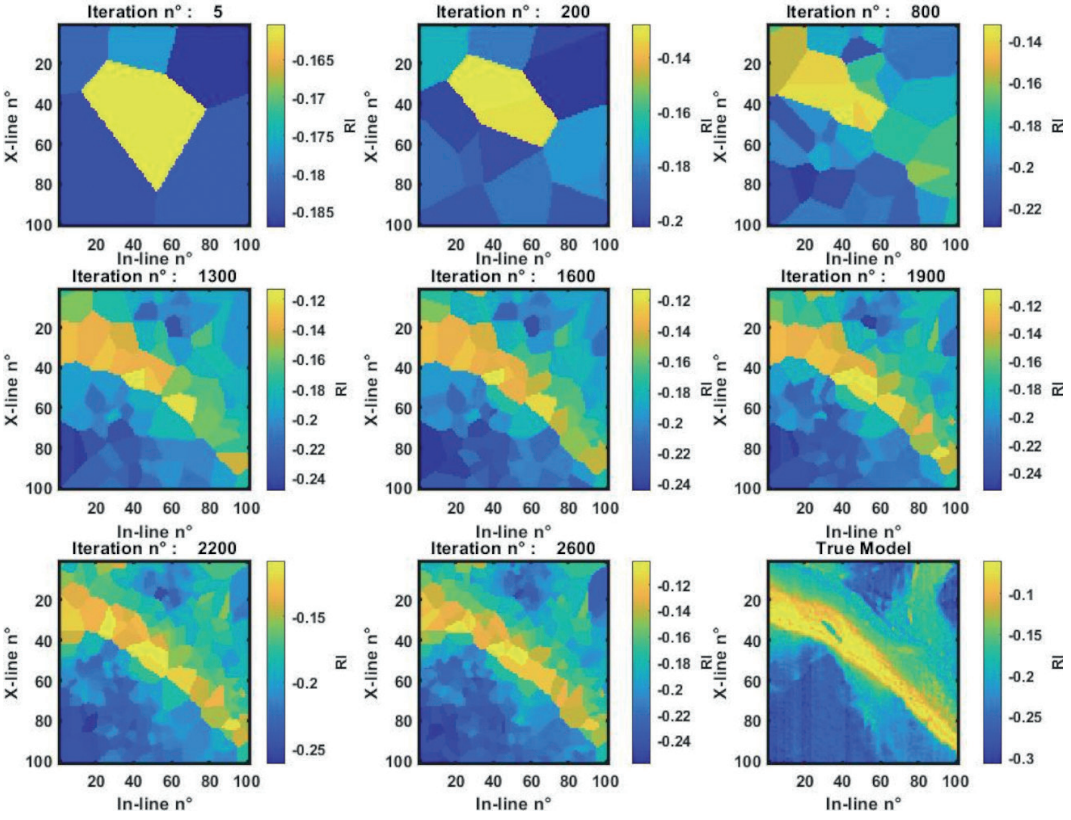

Fig. 2 - Example of evolution of the sampled **RI** models from iteration 5 (top left) to iteration 2600 (bottom center) over a regular spaced grid of 100x100 CDPs. The reference model is shown on the bottom right corner.

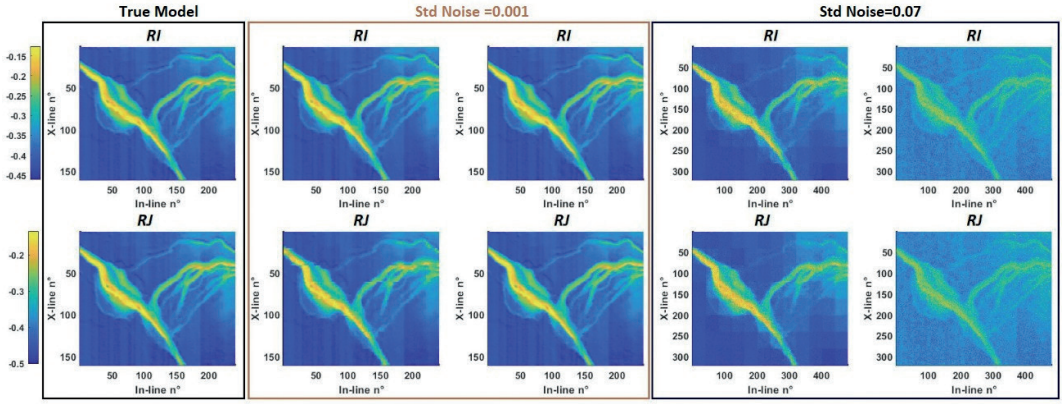

Fig. 3 - Comparison between the reference model and the MAP solutions provided by the rjMCMC and by the standard Bayesian approach for different S/N ratios. RI and RJ represent the relative contrasts in the **Ip** and **Is** values at the reflecting interface, respectively.

within an angle range between 0 and 45 degrees. We considered two scenarios with different S/N ratios and with Gaussian-distributed noise affecting the data. In the first and second case the noise standard deviation is equal to 0.001 and 0.07, respectively. In both cases we use 30 chains each one running for 10000 iterations. The models sampled after 3000 iterations are used to numerically compute the posterior model but for the lack of space only the maximum-a-posteriori (MAP) solution is discussed here. For a high S/N ratio both approaches provide final MAP solutions in good agreement with the reference model and where the formation boundaries can be mapped with high accuracy. Differently, as the noise increases, the standard Bayesian algorithm without lateral constraints provides an estimated model characterized by significant scattering that is produced by the noise propagation from the data to the model space. On the contrary, the implemented rjMCMC algorithm efficiently attenuates the ill-conditioning of the inversion procedure: From the one hand, the averaging of the AVA response within the same Voronoi cell significantly increases the S/N ratio of the observed data. From the other hand, the averaging of the elastic properties estimated for the CDP positions falling within the same cell, inherently introduces lateral constraints into the inversion framework. Both these characteristics of the rjMCMC algorithm ensure a more stable inversion procedure and more reliable results.

Conclusions. We used a reversible jump Markov chain Monte Carlo algorithm (rjMCMC) to include data-driven lateral constraints into target-oriented AVA inversion. The aim of this method is two-fold: increase the S/N ratio of the recorded data and automatically adapt both the parameterization of the subsurface and the lateral model constraints to the lateral variability of the observed data. Synthetic inversion tests under different S/N ratios were used to validate the implemented method and to compare its predictions to those provided by a standard Bayesian inversion algorithm without lateral constraints. Our experiments showed that in case of high S/N ratios both approaches yield similar results. For low S/N ratios the standard Bayesian approach fails to reconstruct the actual subsurface structures and provides a final prediction totally covered by noise. Differently the proposed rjMCMC ensures much more stable and reliable results, in which the lateral elastic discontinuities are accurately recovered. The superior performance of the proposed rjMCMC method is guaranteed by the transdimensional inversion framework that inherently adapts the subsurface parametrization to the lateral variability of the observed data. In other terms the rjMCMC algorithm samples solutions with an appropriate level of complexity to fit the data to statistically meaningful levels. The following step of our research is to apply the implemented algorithm to field data.

References

Aleardi, M., Ciabarri, F., and Gukov, T. (2019). Reservoir Characterization Through Target-Oriented AVA-Petrophysical Inversions with Spatial Constraints. Pure and Applied Geophysics, 176(2), 901-924.

Bodin, T., and Sambridge, M. (2009). Seismic tomography with the reversible jump algorithm. Geophysical Journal International, 178(3), 1411-1436.

Buland, A., and Omre, H. (2003). Bayesian linearized AVO inversion. Geophysics, 68(1), 185-198.

Tetyukhina, D., van Vliet, L. J., Luthi, S. M., and Wapenaar, K. (2010). High-resolution reservoir characterization by an acoustic impedance inversion of a Tertiary deltaic clinoform system in the North Sea. Geophysics, 75(6), O57-O67.

Ursenbach, C. P., and Stewart, R. R. (2008). Two-term AVO inversion: Equivalences and new methods. Geophysics, 73(6), C31-C38.

COMPARISON OF OBJECT FUNCTIONS FOR THE INVERSION OF SEISMIC DATA AND STUDY ON THE POTENTIALITIES OF THE WASSERSTEIN METRIC

L. Stracca, E. Stucchi, A. Mazzotti
Department of Earth Sciences, University of Pisa, Italy

Introduction. The aim of an inverse problem is to find or estimate the unknown parameters of a model, knowing the data it generates and the forward modeling operator that defines the relationship between a generic model and its predicted data. In any inversion process, the main information to update the tested models is given by a certain object function that quantifies the misfit between the observed data to invert and the data predicted by the models themselves. This function has to be defined in order to measure the similarity between the predicted data and the observed ones, in order to drive the inversion procedure towards a satisfying solution, corresponding to the global minimum in the optimal case.

In seismic data inversions, the most chosen object function is the L2 norm of the difference between the predicted and the observed data. This choice is justified by this function's many advantageouses properties, such as: low computational cost, noise insensitivity, high resolution of the results. On the other hand, when applied to oscillating data, this same function is affected by the cycle-skipping problem: the overlap of signal portions with the same polarity (but different phase) generates local minima in the object function's trend. When the starting model chosen at the beginning of the inversion process isn't close enough to the true model, the process may converge to a local minima, returning an incorrect solution to the problem (Virieux and Operto, 2009; Sajeva *et al.,* 2016).

Misfit functions tested. In this study we tested different object functions that may be applied when inverting seismic data. The most important driving criterium for choosing the functions to compare is the possibility to avoid or significantly reduce the cycle-skipping problem. On the basis of the published literature the following objective functions were selected: Instantaneous envelope and phase misfit (Bozdag *et al*., 2011), Adaptive Waveform Inversion (AWI; Warner and Guash, 2016) and quadratic Wasserstein metric (Engquist and Froese, 2014; Yang *et al*., 2018). The most of the attention during the development of this study was given to this last object function, as it was introduced only recently as a potential alternative to the L2 norm in the inversion of seismic data, and seems to perform well against the cycle-skipping. The Wasserstein distance is a transport metric and, given a cost function, computes the minimal value this function may return when a distribution (e.g. one of the predicted traces from a given velocity model) is converted in another one (the corresponding trace in the observed data).